Water and the city: exploring links between urban growth and water demand management

Dimitrios Bouziotas, Evangelos Rozos and Christos Makropoulos

ABSTRACT

Urban water management is currently understood as a socio-technical problem, including both technologies and engineering interventions as well as socioeconomic dimensions and contexts vis-à-vis both end users and institutions. In this framework, perhaps the most important driver of urban water demand, at the intersection between engineering, social and economic domains, is urban growth. This paper examines aspects of the interplay between the dynamics of urban growth and the urban water cycle. Specifically, a cellular automata urban growth model is re-engineered to provide growth patterns at the level of detail needed by an urban water cycle model. The resulting toolkit is able to simulate spatial changes in urban areas while simultaneously estimating their water demand impact under different water demand management scenarios, with an emphasis on distributed technologies whose applicability depends on urban form. The method and tools are tested in the case study of Mesogeia, Greece, and conclusions are drawn, regarding both the performance of the urban growth model and the effectiveness of different urban water management practices.

Key words | cellular automata, decentralised technologies, urban growth, urban water management

Dimitrios Bouziotas
Evangelos Rozos
Christos Makropoulos (corresponding author)
Department of Water Resources and Environmental Engineering,
Faculty of Civil Engineering,
National Technical University of Athens,
Heroon Polytechneiou 5,
Zographou GR-157 80,
Greece
E-mail: *cmakro@mail.ntua.gr*

Christos Makropoulos
KWR, Water Cycle Research Institute,
Groningenhaven 7,
Nieuwegein 3433 PE,
the Netherlands

INTRODUCTION

The demand for long-term infrastructure adaptability in an ever-changing environment is gradually increasing the attention given by researchers and practitioners to more integrated studies that couple socioeconomic and environmental indices with long-term infrastructure planning (Engelen *et al.* 1997; Pataki *et al.* 2011). This evolution is also reflected in water management, where modern practices tend to look into resiliency (Folke 2006) and sustainability issues (Brown *et al.* 2009) while considering a broader range of available distributed technologies, complementing centralised solutions, for managing water within the cities (Makropoulos & Butler 2010). Technologies for managing stormwater locally, such as sustainable urban drainage systems (Makropoulos *et al.* 1999; Woods-Ballard *et al.* 2007), are now becoming much more common, distributed demand management technologies such as greywater recycling (GWR) are emerging (Memon *et al.* 2007) and local rainwater harvesting (RWH), this millennia-old practice, is re-studied (Crouch 1996) and re-introduced (Partzsch 2009).

The emphasis put on sustainability in urban water management raises new questions and challenges, linked to urban planning and points towards the need for an extended interdisciplinary collaboration. This is particularly evident in approaches that attempt to organically integrate elements of sustainable stormwater management into urban planning, such as low-impact development (van Roon 2005) and water-sensitive urban design (Brown & Clarke 2007). Within this context, the perspective of sustainability in urban water management looks more carefully into the localisation of the urban water cycle (van Roon 2007) in addition or even as an alternative to traditional large-scale, central urban water infrastructure. The local scale (neighbourhood or even household) emerges as a key unit with regards to locally based sustainable urban water services (Makropoulos & Butler 2010), and hence a scale of interest for (water sensitive) urban planning. It should be noted that while the transition towards Water-Sensitive Cities (Wong 2007; Brown *et al.* 2009; Bach *et al.* 2012) has begun in the context

doi: 10.2166/hydro.2014.053

of drainage, a long way is still needed to reach the same level of awareness of the interplay between urban planning and water demand or wastewater management.

The paper focuses on this interplay by redeveloping an urban growth model and linking it to an urban water cycle model. The hypothesis is that this coupling will allow us (1) to investigate the impact of alternative water demand management (WDM) practices, taking into account their suitability under specific characteristics of the urban areas for any given 'snapshot' of the city's evolution; and (2) to forecast the long-term evolution of water demand under different urban growth projections simulated using the urban growth model. The first outcome could help detect and prioritise the most suitable intervention practice(s) for the specific areas within the studied region. The second could assist in the development of customised (medium to long term) intervention roadmaps.

INTEGRATING URBAN GROWTH AND URBAN WATER CYCLE MODELS: SCALE AND DATA ISSUES

There exist several practical challenges in the use of urban growth models in an integrated urban water management context. For example, the need for local scale modelling makes typical statistical population models unsuitable to examine links between urban growth and water demand projections within a (necessarily local) water-sensitive urban context. Furthermore, models that involve small-scale geographical components tend to be computationally data-intensive (House-Peters & Chang 2011) and such data often do not exist, or are scattered between government agencies, water companies and other actors. Therefore, there is a need for a parsimonious approach to modelling, applicable to data-scarce environments. While the fusion between urban growth and water cycle localisation in modelling can in principle be addressed through combined, micro-scale simulation models (e.g., UrbanSim (Waddell *et al.* 2003)), such agent-based micro-simulations are particularly data-intensive and computationally heavy. This limits their suitability to data-ample environments (such as the USA or Western Europe), and can be of limited help to areas with great interest par excellence, such as third-world countries with explosive urban growth patterns (Vlachos & Braga 2001). On the other hand, more parsimonious models, such as cellular automata (CA) only provide binary (urban and non-urban) or at best fuzzy (partially urban, with a membership value being assigned to each cell at each time step) classification (Liu 2008). This is problematic as some localised urban water cycle technologies are only applicable to specific housing types (or urban densities). For instance, suburban houses have ample green space, thus enabling the installation of RWH schemes and local sustainable stormwater interventions such as biofiltration trenches, while dense blocks of flats may be more suitable for GWR schemes at the building level. A clear need hence arises for parsimonious urban growth models (to address issues of data scarcity) that can however also provide (some) spatial characteristics at a neighbourhood or housing scale.

To address this problem, we develop a CA model capable of generating raster images of urban growth patterns with cell dimensions equal to the resolution of maps usually provided by EU Agencies (e.g., $100 \times 100\,\mathrm{m}^2$ for CORINE maps). It is argued that this resolution is of particular interest to urban water management applications, since it is close to the spatial scale of the neighbourhood. Cellular automata are a well-known technology for urban modelling (see e.g., White & Engelen 1993, 1997; Couclelis 1997; Clarke *et al.* 1997; Batty 2000), offering a range of unique characteristics that are particularly favourable for spatial applications (Liu 2008), such as simplicity in their modelling structure, proximity to geographic information systems (GIS) and ability to include probabilistic, stochastic or fuzzy transition rules, thus enabling significant modelling flexibility and experimentation.

In this work, the CA model is equipped with fuzzy inference, allowing it to incorporate a level of human reasoning via the use of linguistic rules (Liu & Phinn 2003; Dragicevic 2004; Mantelas *et al.* 2010). The basis for our development is provided by a fuzzy constrained CA model, originating from the work of Mantelas *et al.* (2010). This model is re-engineered to be able to simulate multiple-state cells, instead of binary (e.g., Clarke & Gaydos 1998) or fuzzy (e.g., Liu & Phinn 2003) cell states, thus being able to produce different urban densities and consequently housing units with different properties that can be used as input for localised urban water cycle simulation.

This multiple-state nature of the developed CA model enables a meaningful coupling between urban growth and water cycle management models. Multi-state CA models were initially introduced more than 15 years ago. For example, Engelen *et al.* (1997) applied a CA model to Cincinnati, USA, in order to investigate the capabilities of a multi-state CA modelling framework to realistically simulate observed growth and to generate spatial patterns and clusters of activity at the city scale, with promising results. Since then, multi-state CAs have mostly been used to model more complex urban phenomena, such as traffic flow patterns (Wang & Ruskin 2006) although interest in their use for modelling complex urban dynamics is reviving (Ding *et al.* 2013).

The Urban Water Optioneering Tool (UWOT) (Makropoulos *et al.* 2008; Rozos *et al.* 2010; Rozos & Makropoulos 2013) is employed to model the complete urban water cycle in a bottom-up logic, allowing for the assessment of the impact of distributed water-aware technologies, defined here as technologies that help to improve the performance of the urban water cycle. Such water-aware technologies include low flush toilets, RWH and greywater reuse schemes (Makropoulos & Butler 2010). UWOT is able to simulate both 'standard' urban water flows (potable water, wastewater and runoff) as well as their integration through recycling at a household, neighbourhood or city scale (Rozos & Makropoulos 2012).

It is argued that this combination of a (suitably modified) CA model with UWOT provides a balanced approach between parsimony and output detail which drastically improves over the usual binary CAs by providing indications on the type of housing units, thus increasing insights on the potential for water technology applicability at local and regional scales.

THE BI-PARAMETRIC MULTI-STATE CA MODEL

To study the dynamics of urban development and having integration with UWOT as a key requirement in mind, a fuzzy constrained CA model was developed, based on a simpler, single-state model (Mantelas *et al.* 2010, 2012b). The adopted methodological approach combines fuzzy logic (Zadeh 1965), to incorporate a level of 'reasoning', with CA, to simulate projections of future residential urban growth. The modelling framework is shown in Figure 1 and includes three main stages:

(a) Estimation of the 'suitability factor (SF)' (desirability for urbanisation driven by various spatially related factors, e.g., proximity to transportation network, etc.) of the area with the use of fuzzy logic.
(b) Assessment of the 'initial CA model conditions' (initial urban fabric image), with the aid of available GIS input such as land-cover/land-use data and satellite images.
(c) Execution of the model and 'generation of future urban growth patterns' (in the form of raster maps) for the studied period at an annual time step.

Four independent, parallel, fuzzy inference systems (FIS), each focusing on one distinct set of urban growth factors, was developed and used to calculate the suitability of the studied area for urbanisation. The use of independent FIS leads to a highly configurable mapping, which allows for greater versatility in case more urban growth factors need to be taken into account. The FIS inputs that can be used depend on available data, with physical restrictions (slope, land use and water bodies) and accessibility (transportation network) being of primary importance. In this study the following set of inputs to the FIS were used:

- 'Accessibility' to road networks (including primary and secondary road network, as well as motorway links): areas close to road networks received a high suitability score.
- 'Proximity' to green areas or the sea: areas close to green areas or the sea received a high suitability score.
- 'Slope' of the terrain: areas with mild terrain received a high suitability score.
- 'Availability' of mass transportation, expressed as a distance from main transport hubs: areas close to main transport hubs received a high suitability score.

The outcome of this process was the mapping of inputs to a set of fuzzy values that are then inter-connected through fuzzy rules in order to assess the overall suitability in each inference system. The fuzzy inference rule formation deploys logical operators to link different inputs in the case of multiple-input–single-output systems, e.g., in the

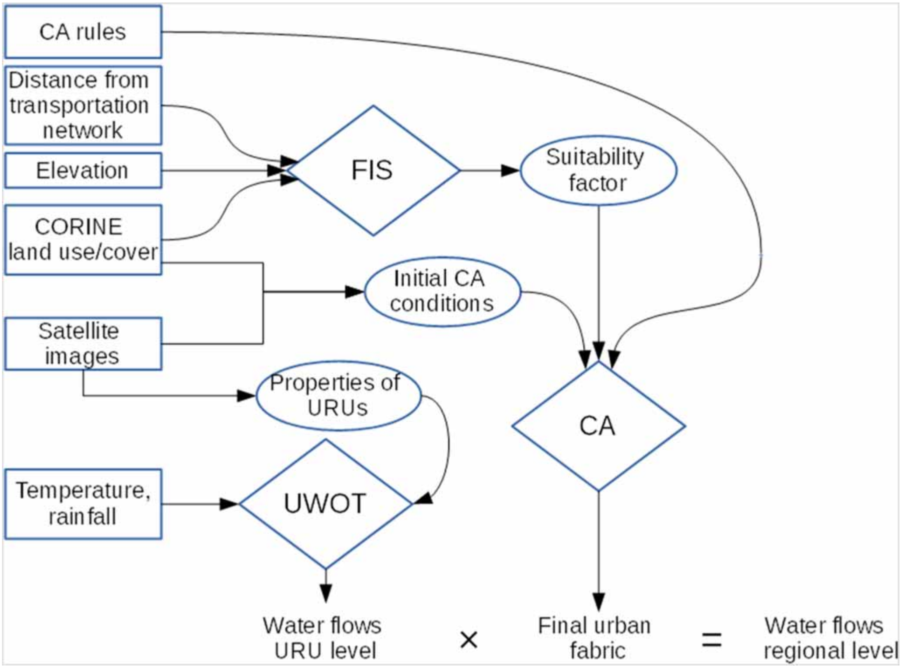

Figure 1 | The flow chart of the interaction of the water management model with the fuzzy constrained CA model. Data are symbolised with rectangles, processes are symbolised with rhombi and intermediate results with ellipses.

case of road network accessibility the following combination of factors was used:

> **IF** 'Primary Road Distance is Small' **AND** 'Motorway Link Distance is Small', **THEN** 'overall suitability is Very High'.

After the implementation of the rules, the fuzzy output values are defuzzified with the use of the centre-of-gravity technique in order to provide the final, crisp values representing the SF, which is related to the desirability for urbanisation driven by the specific input variable(s). The SF values derived from each FIS are then merged (using, in the absence of any differentiating evidence, equal weighting) to obtain the overall SF, for each cell, with values ranging from 0 (completely unsuitable for settlement) to 1 (completely suitable). The final result is a raster map of overall suitability, which in turn is an input for the CA urban growth model. More information about the implementation of fuzzy logic for the calculation of the SF can be found in previous works (Rozos *et al.* 2011; Mantelas *et al.* 2012a).

As discussed above, the urban growth model assumes multiple states of urban growth, which represent varying degrees of urban density. The mechanics behind multiple-state urban growth follow a pattern of cell state allocation and transformation, which comprises the following stages, one at each time step (Figure 2):

- An urban growth algorithm (UGA), similar to the one presented and successfully tested in earlier works (Mantelas *et al.* 2010, 2012b; Rozos *et al.* 2011) decides which non-urban cells are to be urbanised in each time step. Two rules of urban expansion and one rule of 'spontaneous' growth (in areas without neighbouring urban cores) are applied, as suggested by Mantelas *et al.* These rules relate to the binary urban raster map of each time step – in other words, decide between urban and non-urban cell types only.
- The state allocation algorithm (SAA) designates different cell states to all cells which were urbanised with the previous algorithm, based on neighbouring urban pressure and density. This rule applies only to cells that were turned from non-urban to urban at the specific time step.
- An intensification module (INM) assigns denser urban states to existing, urban cells. This allows cells that are already urban to transform into urban states with greater

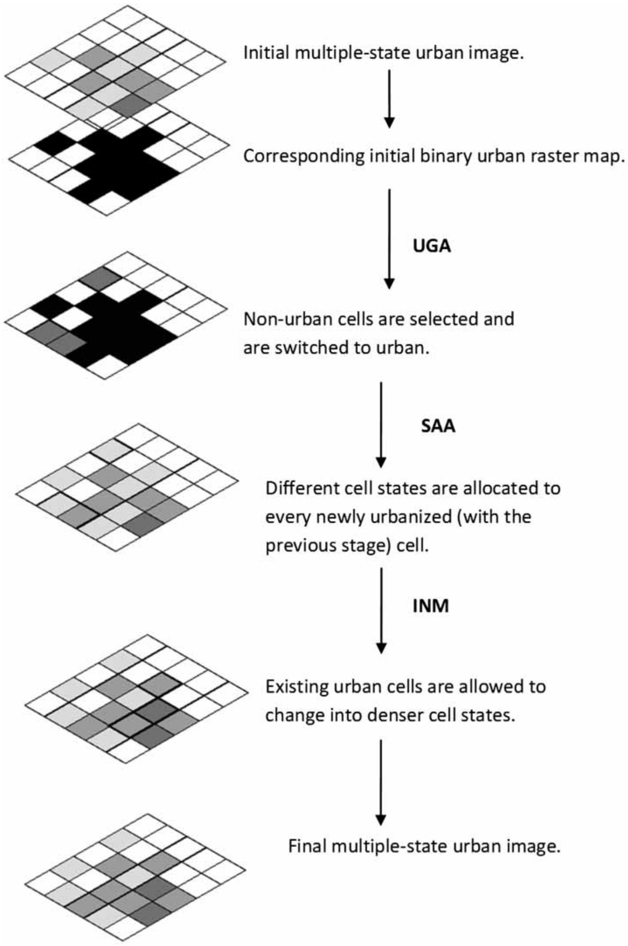

Figure 2 | The framework of cell state transformation and allocation that drives multiple-state urban growth.

urban density. This feature is essential to represent a characteristic transformation of urban areas in Greece, where urban density is generally increased (through a legislative system known as 'antiparochi' – see Mantouvalou & Mavridou 2007) in a single-building basis as single-floor houses with gardens transform into densely built flats within the same, unchanged road network layout.

All rules of transformation within the aforementioned three stages combine the SF with neighbourhood-driven pressure, based on the Moore neighbourhood pattern (Weisstein 2005), with different radii of the Moore neighbourhood being employed by each rule. The rules are all of a probabilistic nature, thus allowing for a more realistic representation of urban growth processes. These rules apply to each cell at each step of the model, taking into account the total amount of urban cells in the neighbourhood, as well as the amount of neighbouring urban cells with specific urban states, with the latter being used in the SAA. The INM also employs rules based on the urban pressure of the neighbourhood (e.g., urban cells with higher cell states lead to higher urban pressure for the specific cells).

Besides the cell neighbourhood effects, a velocity factor (VF) in (0, 1) was implemented in every rule, denoting the intensity with which the rule is applied temporally as well as the different paces of different rules. For example, urban expansion is a relatively fast process compared to intensification, so intensification has a much smaller VF parameter in its rules (see Table 1). In order to define the speed at which each rule is applied, the population dynamics of the area need to be known (i.e., population statistics from census studies need to be known at regular time steps). The VF is then calibrated based on the speed patterns of past population dynamics. The formulae and details for each rule of the case study can be seen in Table 1. All factors are probabilistic in nature and are defined within (0, 1).

The parametric drivers of the rules are the SF and the VF. In principle, both of them can vary spatially and temporally and are subject to calibration. In some studies, the role of SF is two-fold, both representing suitability in an area as well as determining urban growth and densification speed (e.g., Li & Yeh 2000; Mantelas *et al.* 2012a). However, we argue that these factors represent different

Table 1 | The general rule formulation used in the CA model

General rule formula: PROB = SF × MooreRules × VF

	Rule name	Moore neighbourhood radius in MooreRules	VF
UGA	Edge expansion 1	1	0.75
	Edge expansion 2	2	0.68
	Spontaneous growth	3	0.50
SAA	Urban state allocation (2, 3 or 4)	3	–[a]
INM	Intensification, state 2–3	2	0.25
	Intensification, state 3–4	2	0.10

PROB is the probabilistic result of cell state change, SF is the suitability index of the particular cell, MooreRules are urbanisation ratios driven by neighbouring cells and VF is the velocity factor.

[a]Blank: the urban state allocation step allocates states to urbanised cells based only on neighbouring cell states. Hence, a VF factor is needless for this rule.

mechanics of urban growth and have distinct roles. This is why, in our case, a bi-parametric approach was chosen instead, with separate roles between the two parameters; the SF denotes the 'desirability to build in an area', driven by human reasoning, while VF stands for 'speed of building in an area', thus addressing drivers related, for example, to macro-economic variables and with them the temporal evolution of different urbanisation mechanisms, such as urban expansion and intensification. In other words, SF represents a number of socio-geographic factors that make an area desirable, while VF quantifies what drives desirability into action.

Since the socio-geographic factors are unlikely to radically change during short time intervals, SF is expected to exhibit much higher spatial variability than temporal. The opposite stands for VF since speed is directly related to economic growth, population inflow, immigration rates, legislation restrictions and relocation politics, etc. Therefore, in a typical short-term projection case, SF can be a spatially variable, temporally constant matrix, while the opposite can be assumed to be true for the VF. In cases of scarce socioeconomic data, such as this case study, constant VF values can be used, in order to retain a character of simplicity and laconic parameterisation, subject only to general population trends for the area of interest.

Temporally variable SF may be used in cases of what-if scenarios (i.e., exploring the evolution of infrastructure and its impact in the urbanisation of an area) or additional available spatial information over time, such as the detailed evolution of the road network of the area or a dynamic change in land use over specific areas (land reform projects, infrastructure, parks, etc.). On the other hand, VF can be derived through a separate socioeconomic model as an exogenously applied dynamic constraint (if data are available). Obviously, these two factors permit the formation of a number of scenarios, such as new infrastructure and land-use policies (with a change in SF) or population and economic growth projections (with a change in VF).

The bi-parametric rationale offers the capability of both spatial and temporal configuration, thus enhancing the operational flexibility of the model. Temporal configuration is, after all, equally important to a CA model, but is not often addressed, with the majority of CA models allowing a configuration based on the best fitting between given spatial data sets, without any additional temporal calibration features (Liu 2008).

THE CASE STUDY: MESOGEIA, ATHENS

The model was applied in the region of Mesogeia, in the eastern part of Athens, a mostly agricultural area until two decades ago. Then, rapid urban development occurred, resulting in the doubling of its urban cover. Mesogeia is a relatively autonomous region in terms of urban growth (Mantelas *et al.* 2012a) as it is geographically separated from the rest of metropolitan Athens by Mount Hymettus in the west. Furthermore, it constitutes an 'ideal' case of event-driven, peri-urban rapid development, triggered by large-scale infrastructure, due to the fact that it was the location of the 2004 Olympic Games (Couch *et al.* 2007).

To prepare the SF and the initial urban fabric raster image, a series of geospatial manipulations were performed based on available geographic data sets. The CORINE land-cover raster data for the years 1990 and 2000 (Figure 3) were obtained from the European Environment Agency (EEA 2012) and re-projected to the Greek coordinate system HGRS 1987. For the terrain of the studied area, the digital terrain model was obtained from the Hydroscope Project (2011). The transportation network of the area was obtained from OpenStreetMap (2011) and was converted to a raster map containing primary and secondary roads, railway stations and motorway links. Finally, census data were obtained from the Greek National Statistics Agency, ELSTAT (Table 2).

The basis on which key urban growth characteristics and dynamics are identified and outlined were the CORINE data sets. The red areas (darker areas in the black and white version of the image) in Figure 3 carry the CORINE identification code for 'discontinuous urban fabric', comprising residential areas around the edge of urban district centres, and certain urban districts in rural areas. These units consist of blocks of flats, individual houses, gardens, streets and parks, each of these elements having a surface area less than 25 ha. This type of land-cover can be distinguished from continuous urban fabric by the presence of permeable surfaces: gardens, parks, planted areas and non-surfaced public areas (European

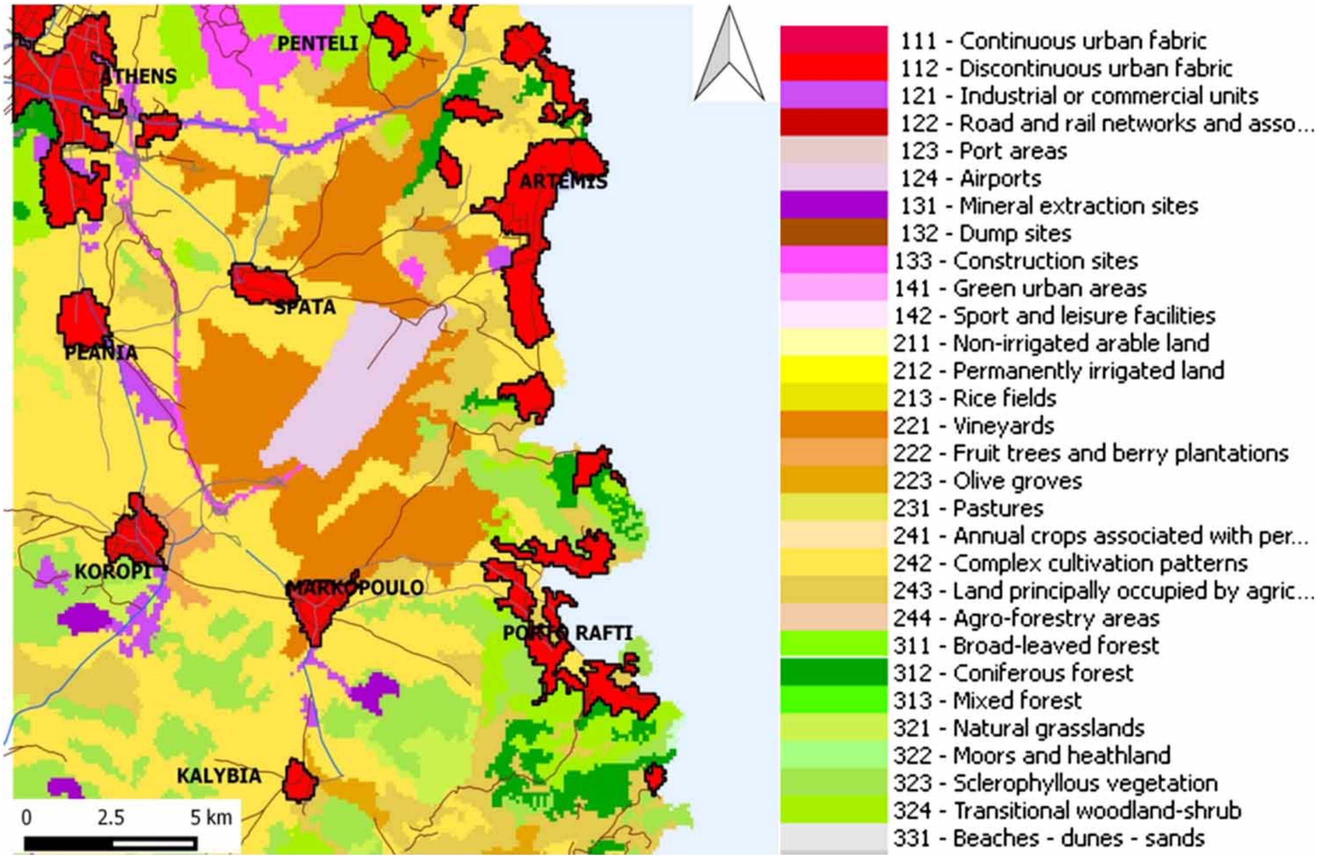

Figure 3 | Land uses and transportation network of the study area (resolution of the raster map is 100×100 m^2) according to CORINE 2000. Coordinates at the centre of the map for EPSG:3,857 are (37.9372, 23.941). Please refer to the online version of this paper to see this figure in colour: http://www.iwaponline.com/jh/toc.htm.

Table 2 | Census data for studied area

	1991	2001	2011
Pallini	10,695	17,232	54,390[a]
Gerakas	8,451	13,990	
Anthousa	2,889	2,389	
Artemis	7,077	14,719	33,800[b]
Spata	7,708	10,419	
Koropi	16,239	24,453	30,340
Marcopoulo	9,356	13,644	20,070
Paiania	9,765	12,997	26,620[c]
Glyka Nera	5,753	6,770	
Rafina	7,632	10,701	19,940[d]
Pikermi	1,262	2,924	

[a]Includes population of Gerakas and Anthousa.
[b]Includes population of Spata.
[c]Includes population of Glyka Nera.
[d]Includes population of Pikermi.

Environmental Agency 2012). Therefore, the red/darker areas could be interpreted as a rough estimation of the borders of urban growth of the study area. The remaining areas are classified according to CORINE as complex cultivations, vineyards, sclerophyllous vegetation and transitional woodland-shrub.

An analysis of the map of population density provided by CORINE (Figure 4) suggests that a reasonable and parsimonious grouping could be based on three major density classes: up to 2,000, from 2,000 to 4,000 and above 4,000 inhabitants per square kilometre. Different urban densities correspond to different urban properties, such as occupancy, number of buildings per cell, pervious and impervious areas, etc. To represent the spatial distribution of the urban densities within the multiple-state urban growth model, three different cell states were mapped onto three different density classes with state '2' being associated with detached,

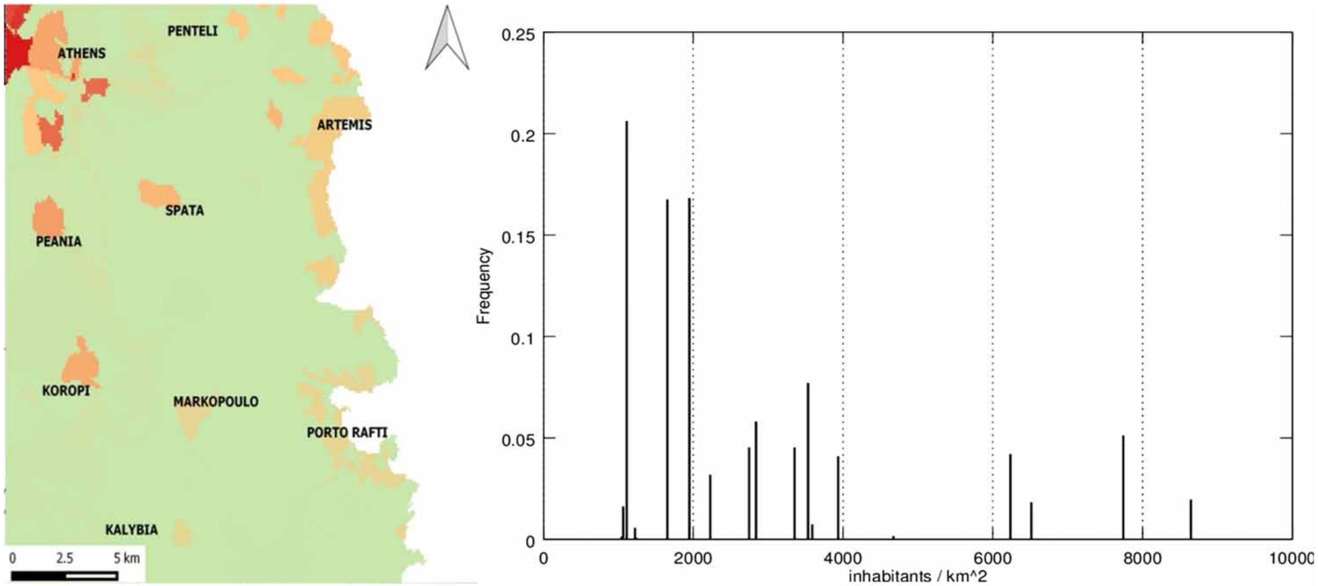

Figure 4 | Left: map of population density distribution according to CORINE 2000 (resolution of raster map is $100 \times 100\ m^2$). Right: frequency of population density values of the CORINE map.

low-storey houses; state '4' with blocks of flats; state '3' with mixed state. State '1' was set to correspond to non-urban cells, while state '0' to cells that cannot be occupied (due to, for example, physical boundaries such as the sea).

The characteristics of each state (average pervious/ impervious areas ratio, number of households, and occupancy) were obtained by manually interpreting satellite images of the study area (Figure 5). Their attributes are given in Table 3. After the state identification, the initial number of urban cells and their spatial distribution inside each residential area were derived by using both the population information from the 1991 census (ELSTAT 2012) and the map of population density disaggregation provided by CORINE (Figure 4, left).

URBAN GROWTH SIMULATION

Using the aforementioned procedure, the initial, multiple-state urban fabric image of 1990 as well as the observed urban fabric image of 2000 was generated. The 2000 image, as well as population time series for each municipality (in this case values for 2000 and 2010) are used to calibrate the model, in terms of both spatial accuracy of

Figure 5 | Satellite images of urban areas ($100 \times 100\ m^2$) of the states (from left to right) 2, 3 and 4, respectively.

Table 3 | Urban density properties of the three states and their corresponding urban response units

	State 2 (low-storey houses)	State 3 (mixed state)	State 4 (blocks of flats)
Occupancy	3.2	7.4	20
Buildings/cell	10	17	15
Urban density (people/cell)	32	125	300
Public impervious (m^2)	1,000	4,645	3,925
Total pervious (m^2)	8,200	2,635	3,225
Building footprint (m^2)	80	160	190

the generated urban patterns and population growth rate. The aim was to reproduce the general urban growth pattern, as well as the population influx for each municipality on the basis of historical population data. As explained before, the SF 0069s was derived using FIS, while the use of the VF is limited to the general population trends due to lack of more detailed data.

The CA model performance is validated against a number of metrics, comprising:

- Cross-tabulation between the modelled and the observed urban cover (based on the CORINE 2000 image) for each municipality.
- Overall population trends in each municipality compared with available census data. Comparing the estimated and observed population influx is essential both for model validation and proper urban water cycle modelling.

The overall spatial performance of the model can be viewed in Figure 6, which shows the CORINE 2000 general urban boundaries (dark grey colour), along with the urbanised cells from the CA model (light grey pixels). White pixels represent cells generated from the CA model that exceed CORINE urban boundaries. It can be suggested that the model performs satisfactorily in all cases of residential zones. It is noted that a number of zones that appear to be without modelled urban cells are characterised by CORINE 2000 data as industrial, commercial or large-scale infrastructure construction zones, so the lack of residential development in these cases does not lead to inaccuracies.

Figure 7 shows the fitting indicators of the model (for each municipality and for the whole area of Mesogeia). The metrics used, viz. the kappa and Lee-Sallee indices (Carletta 1996; Clarke *et al.* 1996) imply that the overall spatial reproduction of urban growth is satisfactory, even with a number of inaccuracies present in certain municipalities, notably Artemis and Marcopoulo. The overall kappa index is 71%,

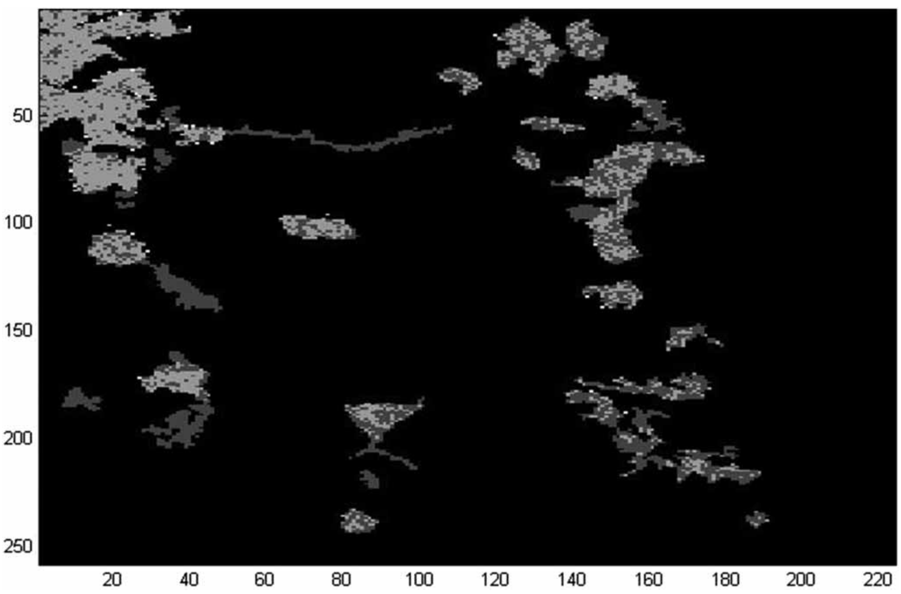

Figure 6 | Overlay of the CORINE 2000 urban boundaries and the simulated residential patterns.

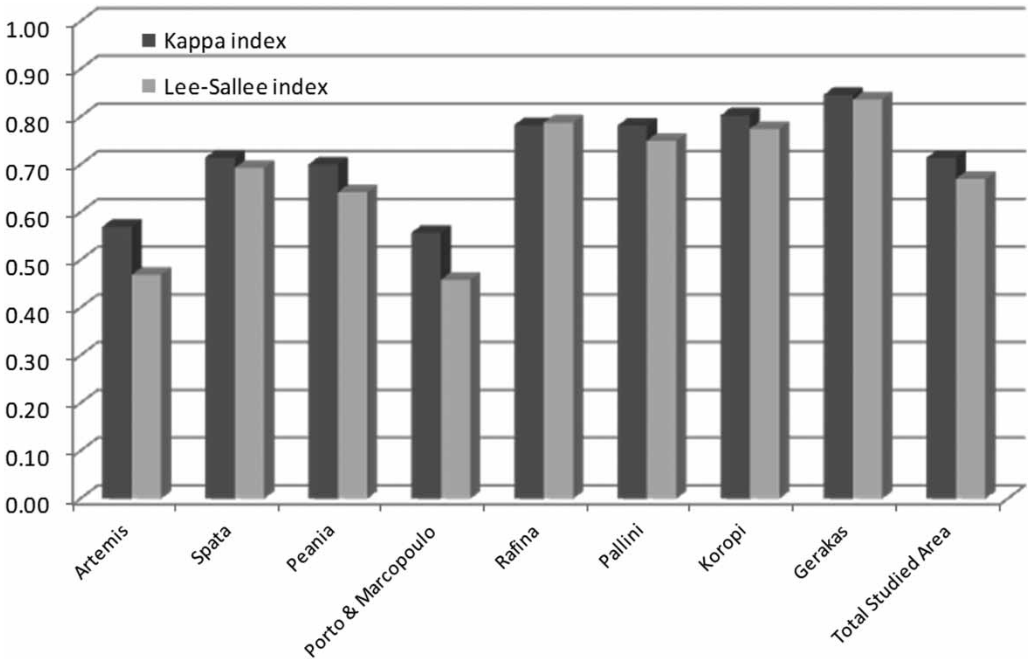

Figure 7 | Fitting indicators for the model results, as compared to the CORINE 2000 urban cover.

which is deemed adequate for an initial application. This is even more so in view of the following two points:

- Detection of land use from CORINE does not provide spatial data with enough accuracy to be fully reliable for elaborate applications such as urban water management at a household level. While CORINE provides a basis for model implementation, one should be aware of its limitations, especially when there is differentiation between different types of land use (Diaz-Pacheco & Gutiérrez 2013).
- A significant part of observed urban growth can be attributed to uses other than residential construction (for instance, commercial or industrial uses) or mixed uses, which is quite common in Athens.

In view of this, the model evaluation was also based on population trends per municipality. This evaluation metric was chosen as a validation measure supplementing spatial metrics, since it is directly linked to water demand and detailed census data were available. In fact, this step is considered essential in the evaluation of the model, as remote sensing cannot substitute but only complement traditional socioeconomic indices (Besussi et al. 2010). Thus, a coupling approach of remote sensing data with socioeconomic indices becomes important at finer scales.

A comparison between observed and simulated population growth (Table 4) shows that the CA model

Table 4 | Observed and simulated population growth for each municipality

Year		1990	2000	2010	2020
Artemis	Census data	7,077	14,719	33,800[a]	
	Simulated	8,640	14,980	24,963	35,216
Spata	Census data	7,708	10,419		
	Simulated	7,171	13,019	19,653	26,615
Peania	Census data	9,765	12,997	26,620[a]	
	Simulated	9,309	15,171	24,208	27,642
Porto Rafti and Makropoulo	Census data	9,356	13,644	20,070	
	Simulated	7,770	12,903	22,137	38,508
Rafina	Census data	6,370	7,777	13,165	
	Simulated	6,493	9,323	11,472	15,450
Pallini	Census data	10,695	17,232	54,390[a]	
	Simulated	9,600	14,125	21,050	23,122
Koropi	Census data	16,239	24,453	30,340	
	Simulated	15,900	19,047	25,300	32,212

[a]This value reflects a growth in municipal borders after new legislation measures. Actual corresponding size (with the same borders as 2000) is expected to be 20–25% smaller.

adequately represents occupancy influx and growth rate in most municipalities. Even nonlinear population trends are represented satisfactorily, with the exception of Pallini, where the model fails to represent the explosive population growth pattern. This case, however, is very complicated since the municipality borders changed between 2000 and 2010 and hence population numbers are not directly comparable.

INTEGRATING THE URBAN WATER CYCLE MODEL

The detailed urban growth projections with multiple states given by the CA model allow the simulation of the total urban water cycle through UWOT at a neighbourhood-level (cellular level) basis. The urban water cycle of each of the three urban states (2, 3 and 4) is modelled in UWOT with the help of what is defined here as the urban response units (URU). We define an URU as a neighbourhood unit with the same size as a single cell ($100 \times 100\ m^2$), characterised by the following properties:

- The number of households: each URU includes a fixed number of identical households. Every household is considered as a structurally independent residential unit with a single connection to the mains.
- The occupancy of the household: this is the average number of people inhabiting a household, which may include a single family or many families in case of multi-storey buildings (URUs that correspond to states 3 and 4).
- The private and public pervious areas (areas occupied by gardens and parks), as well as the private and public impervious areas (road, pavements and rooftops).
- The urban water network configuration: this refers to the installed water appliances, the existence of any water recycling scheme, the type of sewers (combined/separate), etc.

The first three properties, which relate to the urban density of an URU (i.e., are defined by the urban state), are obtained from satellite images (see Table 3). The fourth property comprises all local water-saving or recycling schemes applicable in the particular neighbourhood. In this study, five different network configurations were employed:

- The first two configurations include the business as usual (BAU) scenario as well as the installation of low-water consumption appliances (LOW). These two have identical connections between the water components. The specifications of the in-house water appliances and frequencies of use for both configurations are obtained from the literature (EEA 2001; Grant 2002, 2006; Eartheasy 2012; ENERGY STAR 2012a, 2012b). The daily per capita consumption of the conventional scenario is 184 L/p/d, while in the case of low-water consumption appliances it is reduced to 97 L/p/d.
- The next two configurations attempt to achieve additional water saving by implementing a RWH scheme, as well as its combination with low consumption appliances in the second case (RWHLOW). The tank capacities used in the RWH scheme are dependent on the building type and are assumed to be 2, 10 and 20 m^3 for the states 2, 3 and 4, respectively. The RWH areas of the three states are 80, 160 and 190 m^2 (average roof area estimated from satellite images). The average annual rainfall depth, as estimated from daily rainfall timeseries (FreeMeteo 2011) is 376 mm.
- The fifth configuration includes local GWR (Figure 8) with a local treatment unit that treats water from the shower and hand basin, and supplies treated water to the toilet, washing machine and for watering the garden. The RWH, RWHLOW and GWR configurations differ from BAU and LOW, since they include a tank, which receives harvested rainwater in the RWH schemes or treated greywater from a local treatment unit in the GWR configurations. A more detailed description of the simulation of RWH and GWH schemes can be found in Rozos *et al.* (2010).

In order to assess the demand of the in-house water appliances a series of micro-components are employed (with each micro-component simulating a water appliance), which are then aggregated to calculate the potable water demand of the URU (see Rozos & Makropoulos (2013) for more information on how UWOT accomplishes this). Outputs of all appliances are aggregated and this flow is multiplied with the number of households per cell, which gives the wastewater (WW) charge of the URU. For

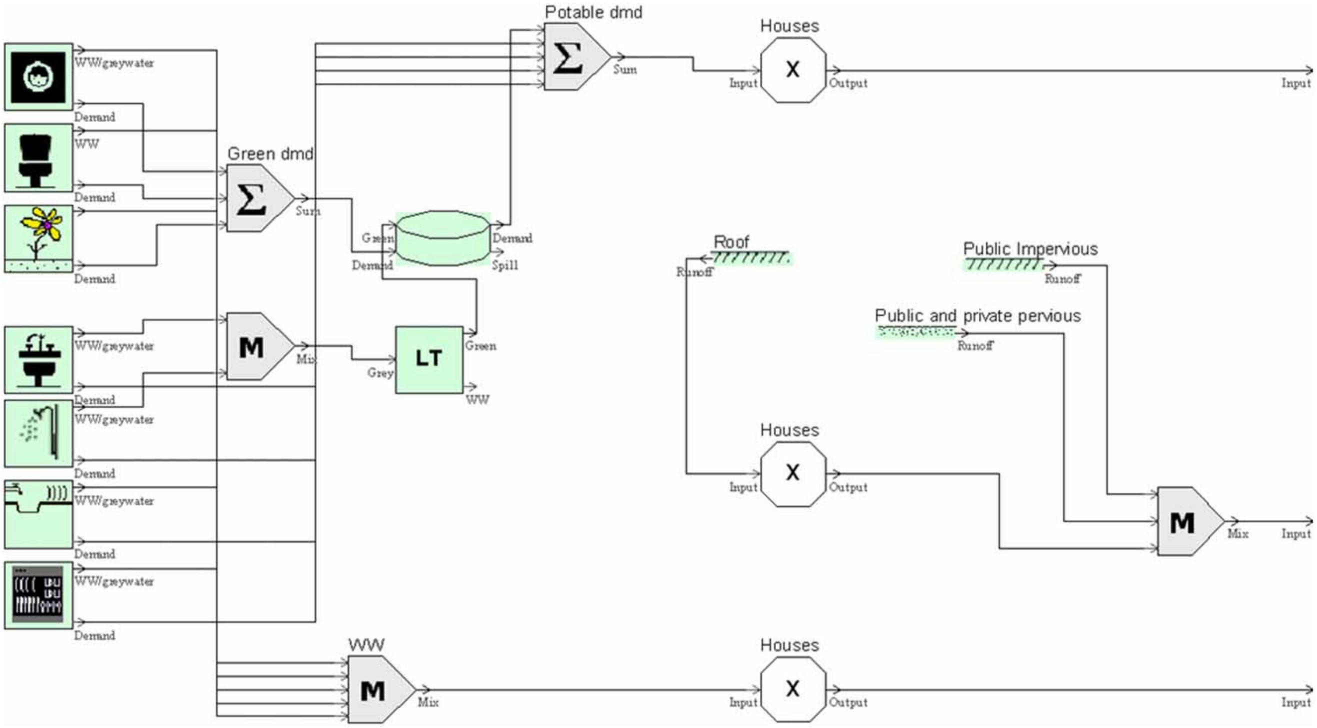

Figure 8 | Indicative network topology of the GWR configuration, modelled in UWOT.

outdoor uses a constant value given by Grant (2006) was used regardless of the urban density. Finally, the rainfall on the roofs of households generates runoff, which, after being multiplied by the number of households, is added to the runoff from the public impervious areas and the total pervious area of the cell, resulting in an estimation of total runoff.

The combination of the five network configurations with the three urban states (Table 3) results in 15 URUs, depicting the full range of feasible technologies at the neighbourhood level for every possible urban state. The urban water cycle of these URUs is then simulated (Table 5), with the use of a daily time step (historical daily rainfall timeseries were obtained from FreeMeteo (2011)) with the simulation period extending from 1 January 1980 to 31 December 1999. The values displayed in this table include average potable water demand, WW and maximum runoff volume (generated from the rainfall on the simulated urban area) for the simulation period.

To obtain the urban water cycle flows at the scale of a municipality for each one of the years 1990, 2000, 2010 and 2020, and assuming no interdependencies between cells in terms of water flows, Table 5 was multiplied with the corresponding number of urban cells per state (see also Figure 1).

Table 5 | Results of simulations of the 15 (3 × 5) urban response units with urban water optioneering tool

		State 2	State 3	State 4
Average potable demand (L/d)	BAU	5,893	22,778	53,873
	LOW	3,091	11,760	27,599
	RWH	5,305	20,574	51,527
	RWH LOW	2,567	9,640	25,259
	GWR	4,165	15,985	37,673
Average WW out (L/d)	BAU	5,718	22,481	53,610
	LOW	2,916	11,463	27,336
	RWH	5,718	22,480	53,610
	RWH LOW	2,916	11,463	27,336
	GWR	3,990	15,687	37,410
Max runoff volume (L/d)	BAU	307,806	866,066	806,880
	LOW	307,806	866,066	806,880
	RWH	297,030	724,577	502,743
	RWH LOW	300,893	739,763	538,959
	GWR	307,806	866,066	806,880

RESULTS AND DISCUSSION

The coupling of UWOT with an urban growth model (albeit a second level coupling according to Brandmeyer & Karimi (2000)) presented here, allows for an assessment of the impact of urban growth on the urban water cycle. It also quantifies the effects of various water-saving technologies at a regional level. For example, Figure 9 shows the evolution of the potable water demand and the indicative maximum runoff volume for each municipality of the study area for the BAU configuration. The improvement of the urban water cycle performance by implementing each one of the four WDM measures compared to the BAU configuration is shown in Figure 10 for Koropi and Artemis (representative municipalities for high and low urban density, respectively), regarding Figure 10(a) potable water demand, Figure 10(b) wastewater volume and Figure 10(c) maximum runoff volume. The results of applying RWH are shown in Figure 11. The evolution of the overall potable water demand of the study area for all four WDM configurations is shown in Figure 12 (contrasted with the BAU configuration). This figure assumes a steady technology uptake rate in existing households of 10% per year.

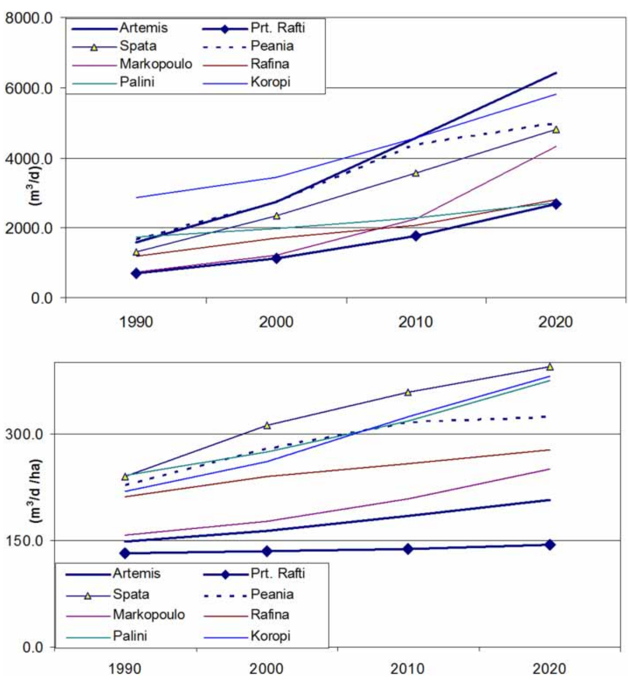

Figure 9 | Indicative potable water demand per day (upper) and maximum runoff volume per hectare (lower) for each municipality of Mesogeia, BAU configuration.

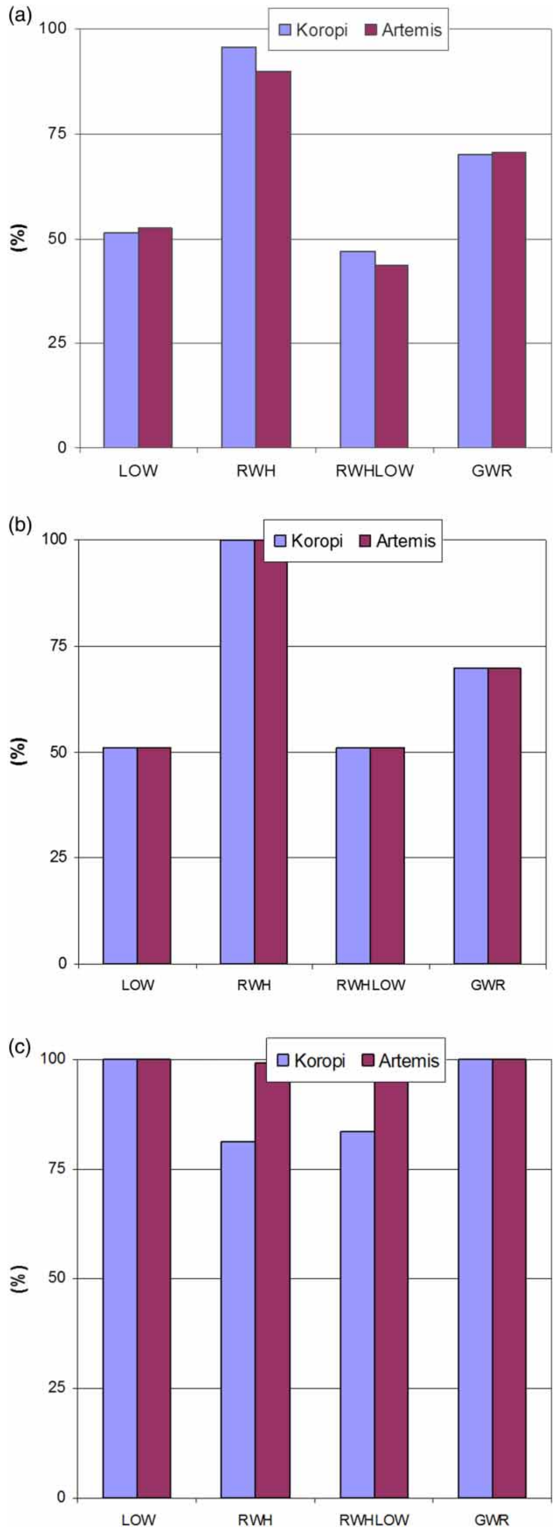

Figure 10 | Potable water demand (a), wastewater volume (b) and runoff volume (c) for each WDM measure, presented as % of the BAU configuration, for the municipalities of Koropi and Artemis.

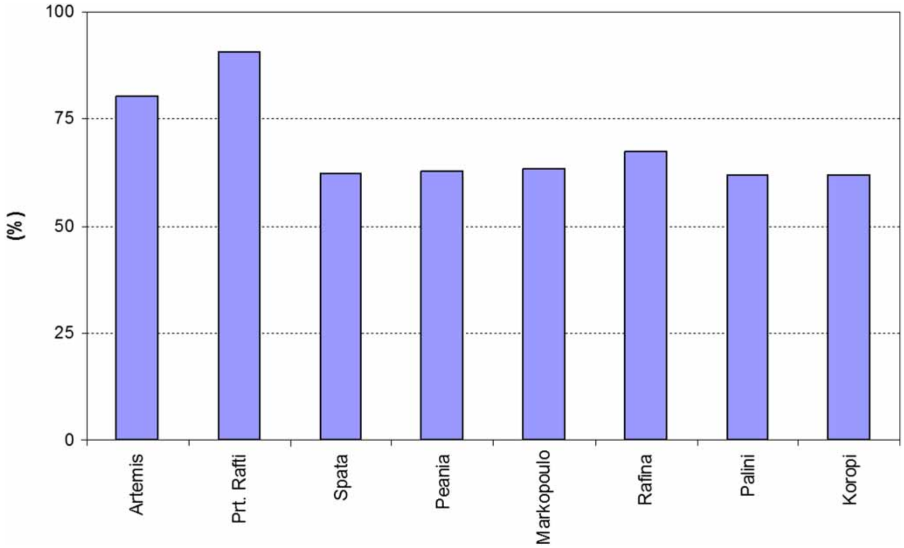

Figure 11 | Runoff volume per municipality for the RWH configuration, presented as % of the BAU configuration.

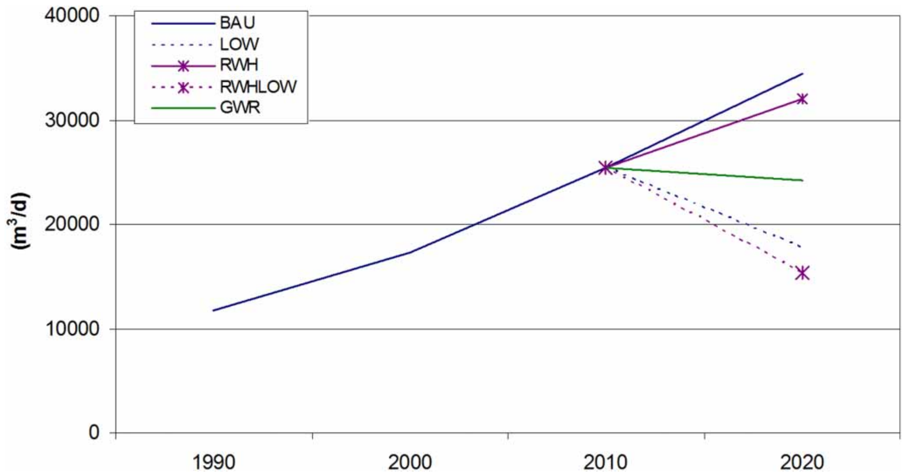

Figure 12 | Comparison of the evolution of potable water demand over the whole study area for the different WDM measures.

With that level of output detail, produced by a bottom-up modelling philosophy, key conclusions can be drawn regarding the effectiveness and, therefore, prioritisation of relevant WDM measures in the studied area, both for more detailed and regional scales:

- Prioritisation of WDM measures in Mesogeia, Athens: the installation of low-water consumption appliances is the WDM measure that achieved the highest reduction of potable water demand (see Figure 10), with GWR achieving a moderate effect. Although this depends on the particular technology mix chosen for testing, all technologies examined are readily available 'off the shelf'. RWH achieved a runoff volume reduction up to 40% in the dense urban areas whereas the reduction is limited to 10% at the low urban density areas. The results also underline the beneficial coupling effect of these WDM, as any simultaneous application of measures enables the synthesis of their individual benefits. The most characteristic example is the installation of the combination of low-water consumption appliances with RWH to reduce both potable water demand and runoff volume (up to 53 and 33%, respectively, in dense urban areas). It should be noted at this point that outdoor water demand is, in fact, dependent on urban form and density (e.g., garden irrigation in low density urban areas) and hence the assumption of a constant outdoor demand made here is a simplification. However, it could be argued that this simplification does not have significant impact on our particular case. If a more realistic estimation of outdoor demand was employed instead, arguably, the performance of LOW, which ranked first, would have remained unaffected, the performance of GWR would have decreased proportionally to the additional irrigation demand while the performance of RWH, which ranked last, would have decreased both because of the additional demand and because of the fact that the peak of this demand is during the summer period when precipitation is at a minimum. Nevertheless, more detailed approaches with respect to calculations of outdoor water demand (such as the one described in Rozos *et al.* 2013) should be used in cases where RWH is expected to be more efficient (e.g., in wet climatic conditions).

- Prioritisation and temporal analysis of demands: if the capacity of the existing regional centralised water system (either to supply water, treat wastewater or convey runoff) is expected to be exceeded by the BAU scenario of the projected urban growth then water can become a limiting factor to urban growth. In this case, measures need be taken well in advance using realistic technology uptake and penetration rates. In such a context, the proposed methodology can lead to the formation of charts of water demand evolution for alternative urban growth projections and WDM measures (such as Figure 12) that can be used to plan intervention strategies (roadmaps) and form adaptation policies as the urban area of study evolves. For the preparation of such a roadmap, it should be clear that the accuracy of the forecasts provided by our method is limited by the uncertainty related to the VF. In this study a constant VF was used, which was calibrated based on past population dynamics. This approach presupposes that the socioeconomic conditions during the forecast period remain similar to that of the calibration period. A more sophisticated approach could entail the employment of a socioeconomic model to estimate the VF at each step of the simulation. This would represent, for example, the periods of increased construction activity and the periods of economic relapse when such activity is decreased.

CONCLUSIONS

The study demonstrated the coupling of urban growth modelling (a CA model) with UWOT for the purposes of planning distributed, site-specific water management interventions at the regional or city level, both as at any given point in time and, potentially, as a roadmap of interventions following the city's evolution. It is argued that this type of work could form a basis for deeper integration between urban design and water management, thus leading to more water-sensitive urban planning policies and mitigation strategies. While the coupling methodology addresses only a cause–effect relationship between urban growth and water impact, more dynamic links are evident through the framework; for instance, the CA model can be calibrated to include spatiotemporal changes induced by water-aware urban planning (e.g., blue-green infrastructure, see Rozos *et al.* 2013) or policies that favour specific, low-impact land use. Such links have not been addressed here, but form the ambition of ongoing work. It is finally suggested that the integration of UWOT with urban growth models at a cell level allows for the investigation of even more sophisticated cases, where certain housing units decide to retrofit technologies or adopt new ones while the urban area is evolving, linked for example to changes in income growth and distribution, awareness raising campaigns, rebate and other supporting policies or even population dynamics and characteristics and hence provide policy-makers at the city level with long-term scenario planning tools for more sustainable water infrastructure.

ACKNOWLEDGEMENTS

The research leading to these results has received funding from the European Union Seventh Framework Programme

(FP7/2007-2013) under grant agreement No. 265122 (Transitions to the Urban Water Services of Tomorrow – TRUST). This publication reflects only the authors' views and the European Union is not liable for any use that may be made of the information contained therein.

REFERENCES

Bach, P. M., McCarthy, D. T., Urich, C., Sitzenfrei, R., Kleidorfer, M., Rauch, W. & Deletic, A. 2012 DAnCE4Water's BPM: a planning algorithm for decentralised water management options. In: *Proceedings of the Ninth International Conference on Urban Drainage Modelling*, Belgrade, Serbia.

Batty, M. 2000 Geocomputation using cellular automata. In: *Geocomputation* (S. Openshaw & R. J. Abrahart, eds). Taylor and Francis, London, UK, pp. 95–126.

Besussi, E., Chin, N., Batty, M. & Paul, L. 2010 The structure and form of urban settlements. In: *Remote Sensing of Urban and Suburban Areas* (T. Rashed & C. Jürgens, eds). Springer, Dordrecht, the Netherlands.

Brandmeyer, J. E. & Karimi, H. A. 2000 Coupling methodologies for environmental models. *Environ. Modell. Software* **15** (5), 479–488.

Brown, R. & Clarke, J. 2007 *Transition to Water Sensitive Urban Design: The Story of Melbourne, Australia*. http://www.tudelft.org/fileadmin/UD/MenC/Support/Internet/TU_Website/TU_Delft_portal/Onderzoek/Kenniscentra/Delft_Research_Centres/Water/Water_News/Water_Dossiers/W_Man/Articles_2007/doc/Presentation_Rebekah_Brown.pdf (accessed 4 February 2013).

Brown, R. R., Keath, N. & Wong, T. H. F. 2009 Urban water management in cities: historical, current and future regimes. *Water Sci. Technol.* **59** (5), 847–855.

Carletta, J. 1996 Assessing agreement on classification tasks: the kappa statistic. *Comput. Linguist.* **22**, 249–254.

Clarke, K. C. & Gaydos, L. J. 1998 Loose-coupling a cellular automaton model and GIS: long-term urban growth prediction for San Francisco and Washington/Baltimore. *Int. J. Geogr. Inf. Sci.* **12**, 699–714.

Clarke, K. C., Hoppen, S. & Gaydos, L. 1996 Methods and techniques for rigorous calibration of a cellular automaton model of urban growth. In: *Third International Conference/Workshop on Integrating GIS and Environmental Modeling. 21–25 January*, Sante Fe, NM, USA.

Clarke, K. C., Gaydos, L. & Hoppen, S. 1997 A self-modifying cellular automaton model of historical urbanization in the San Francisco Bay area. *Environ. Plan. B* **24**, 247–261.

Couch, C., Petschel-Held, G. & Leontidou, L. 2007 *Urban Sprawl in Europe*. Blackwell Publishing Ltd, Oxford, UK.

Couclelis, H. 1997 From cellular automata to urban models: new principles for model development and implementation. *Environ. Plan. B Plan. Des.* **24**, 165–174.

Crouch, D. C. 1996 Avoiding water shortages: some Ancient Greek solutions. In: *Diachronic Climatic Impacts on Water Resources with Emphasis on Mediterranean Region* (A. N. Angelakis & A. S. Issar, eds). Springer-Verlag, Heidelberg, Germany, pp. 129–159.

Diaz-Pacheco, J. & Gutiérrez, J. 2013 Exploring the limitations of CORINE land cover for monitoring urban land-use dynamics in metropolitan areas. *J. Land Use Sci.* **9** (3), 243–259.

Ding, W. J., Wang, R. Q., Wu, D. Q. & Liu, J. 2013 Cellular automata model as an intuitive approach to simulate complex land-use changes: an evaluation of two multi-state land-use models in the Yellow River Delta. *Stoch. Env. Res. Risk A* **27** (4), 899–907.

Dragicevic, S. 2004 Coupling fuzzy sets theory and GIS-based cellular automata for land-use change modeling. In: *IEEE Annual Meeting of the Fuzzy Information, 2004*. Processing NAFIPS' 04, Banff, Albert, Canada, June 2004. Vol. 1, pp. 203–207.

Eartheasy. 2012 *Solutions for Sustainable Living, Low-Flow Aerators/Showerheads*. http://eartheasy.com/live_lowflow_aerators.htm.

EEA 2001 *Sustainable Water Use in Europe: Part 2 – Demand Management, Environmental Issue Report No. 19*. European Environment Agency, Copenhagen, Denmark.

ELSTAT. 2012 *Hellenic Statistical Authority, Dataset Population/Demographic Data*. http://www.statistics.gr/portal/page/portal/ESYE/PAGE-database.

ENERGY STAR. 2012a *Clothes Washers for Consumers*. http://www.energystar.gov/index.cfm?fuseaction=find_a_product.showProductGroup&pgw_code=CW.

ENERGY STAR. 2012b *Dishwashers for Consumers*. http://www.energystar.gov/index.cfm?fuseaction=find_a_product.showProductGroup&pgw_code=DW.

Engelen, G., White, R. & Uljee, I. 1997 Integrating constrained cellular automata models, GIS and decision support tools for urban planning and policy making. In *Decision Support Systems in Urban Planning* (H. P. J. Timmermans, ed.). E&FN Spon, London, UK, Chap. 8, pp. 125–155.

EEA 2012 CORINE land cover: part II.1 Nomenclature. http://www.eea.europa.eu/en/publications/COR0-part2/land_coverPart2.1.pdf.

Folke, C. 2006 Resilience: the emergence of a perspective for social–ecological systems analyses. *Global Environ. Change* **16** (3), 253–267.

FreeMeteo. 2011 Daily weather history for ATHINAI (AIRPORT). http://freemeteo.com/.

Grant, N. 2002 Water closets: valves or syphons, Green Product News – Celebrating sustainable construction products! Autumn 2002, pp. 12–14.

Grant, N. 2006 Water conservation products. In: *Water Demand Management* (D. Butler & F. A. Memon, eds). IWA Publishing, London, UK, pp. 82–106.

House-Peters, L. & Chang, H. 2011 Urban water demand modeling: review of concepts, methods, and organizing principles. *Water Resour. Res.* **47** (5), W05401.

Li, X. & Yeh, A. G. -O. 2000 Modelling sustainable urban development by the integration of constrained cellular automata and GIS. *Int. J. Geogr. Inf. Sci.* **14**, 131–152.

Liu, Y. 2008 *Modelling Urban Development with Geographical Information Systems and Cellular Automata*, 1st edn. CRC Press, Boca Raton, FL, USA.

Liu, Y. & Phinn, S. R. 2003 Modelling urban development with cellular automata incorporating fuzzy-set approaches. *Comput. Environ. Urban Syst.* **27**, 637–658.

Makropoulos, C. K. & Butler, D. 2010 Distributed water infrastructure for sustainable communities. *Water Resour. Manage.* **24**, 2795–2816.

Makropoulos, C. K., Butler, D. & Maksimovic, C. 1999 GIS supported evaluation of source control applicability in urban areas. *Water Sci. Technol.* **39** (9), 243–252.

Makropoulos, C. K., Natsis, K., Liu, S., Mittas, K. & Butler, D. 2008 Decision support for sustainable option selection in integrated urban water management. *Environ. Modell. Software* **23**, 1448–1460.

Mantelas, L., Hatzichristos, T. & Prastacos, P. 2010 A fuzzy cellular automata modeling approach–accessing urban growth dynamics in linguistic terms. In: *Computer Science and Its Applications – ICCSA 2010*, Fukuoka, Japan, 140–151.

Mantelas, L., Prastacos, P., Hatzichristos, T. & Koutsopoulos, K. 2012a A linguistic approach to model urban growth. *Int. J. Agric. Environ. Inf. Syst.* **3**, 35–53.

Mantelas, L., Prastacos, P., Hatzichristos, T. & Koutsopoulos, K. 2012b Using fuzzy cellular automata to access and simulate urban growth. *GeoJournal* **77**, 13–28.

Mantouvalou, M. & Mavridou, M. 2007 Processes of social integration and urban development in Greece. *Antipode*, 191–205. http://courses.arch.ntua.gr/fsr/141020/MantouvalouSocialIntegration-2.pdf (accessed 20 March 2014).

Memon, F. A., Zheng, Z., Butler, D., Shirley-Smith, C., Lui, S., Makropoulos, C. & Avery, L. 2007 Life cycle impact assessment of greywater recycling technologies for new developments. *Environ. Monit. Assess.* **129**, 27–35.

Partzsch, L. 2009 Smart regulation for water innovation – the case of decentralized rainwater technology. *J. Clean. Prod.* **17**, 985–991.

Pataki, D. E., Boone, C. G., Hogue, T. S., Jenerette, G. D., McFadden, J. P. & Pincetl, S. 2011 Socio-ecohydrology and the urban water challenge. *Ecohydrology* **4**, 341–347.

Rozos, E. & Makropoulos, C. 2012 Assessing the combined benefits of water recycling technologies by modelling the total urban water cycle. *Urban Water J.* **9** (1), 1–10.

Rozos, E. & Makropoulos, C. 2013 Source to tap urban water cycle modelling. *Environ. Modell. Software* **41**, 139–150.

Rozos, E., Makropoulos, C. & Butler, D. 2010 Design robustness of local water-recycling schemes. *J. Water Resour. Plan. Manage.* **136**, 531–538.

Rozos, E., Baki, S., Bouziotas, D. & Makropoulos, C. 2011 Exploring the link between urban development and water demand: the impact of water-aware technologies and options. In: *Computing and Control for the Water Industry (CCWI)* (D. Savic, Z. Kapelan & D. Butler, eds). University of Exeter, Exeter, UK.

Rozos, E., Makropoulos, C. & Maksimovic, C. 2013 Rethinking urban areas: an example of an integrated blue-green approach. *Water Sci. Technol. Water Supply* **13** (6), 1534–1542.

Van Roon, M. 2005 Emerging approaches to urban ecosystem management: the potential of low impact urban design and development principles. *J. Environ. Assess. Policy Manage.* **7**, 125–148.

Van Roon, M. 2007 Water localisation and reclamation: steps towards low impact urban design and development. *J. Environ. Manage.* **83**, 437–447.

Vlachos, P. E. & Braga, P. B. 2001 The challenge of urban water management. In: *Frontiers in Urban Water Management, Deadlock or Hope?* (C. Maksimovic & J. A. Tejeda-Guibert, eds.). IWA Publishing, London, UK, pp. 1–34.

Waddell, P., Borning, A., Noth, M., Freier, N. & Ulfarsson, G. 2003 Microsimulation of urban development and location choices: design and implementation of UrbanSim. *Networks Spat. Econ.* **3**, 43–67.

Wang, R. & Ruskin, J. 2006 Modelling traffic flow at multi-lane urban roundabouts. *Int. J. Mod. Phys.* **17** (5), 693–710.

Weisstein, E. W. 2005 Moore neighborhood. *MathWorld–A Wolfram Web Resource*. http://mathworld.wolfram.com/MooreNeighborhood.html.

White, R. & Engelen, G. 1993 Cellular automata and fractal urban form: a cellular modelling approach to the evolution of urban land-use patterns. *Environ. Plan. A* **25**, 1175–1199.

White, R. & Engelen, G. 1997 Cellular automata as the basis of integrated dynamic regional modelling. *Environ. Plan. B Plan. Des.* **24**, 235–246.

Wong, T. H. F. 2007 Water sensitive urban design – the journey thus far: actions towards sustainable outcomes. *Aust. J. Water Resour.* **10** (3), 213–222.

Woods-Ballard, B., Kellagher, R., Martin, P., Jefferies, C., Bray, R. & Shaffer, P. 2007 *The SUDS Manual*. CIRIA, London, UK. http://www.persona.uk.com/A47postwick/deposit-docs/DD-181.pdf (accessed 4 February 2013).

Zadeh, L. A. 1965 Fuzzy sets. *Inf. Control* **8**, 338–353.

First received 24 April 2014; accepted in revised form 3 November 2014. Available online 4 December 2014